

A FERROELECTRIC FAST REACTIVE TUNER (FE-FRT) TO COMBAT MICROPHONICS*

N. Shipman, J. Bastard, M. Coly, F. Gerigk, A. Macpherson, N. Stapley,
CERN, Geneva, Switzerland

I. Ben-Zvi, Brookhaven National Laboratory, Upton NY, USA

C. Jing, A. Kanareykin, Euclid Techlabs LLC, Gaithersburg MD, USA

G. Burt, A. Castilla, Lancaster University, Lancaster, UK

E. Nenasheva, Ceramics Ltd, St.Petersburg, Russia

Abstract

FerroElectric Fast Reactive Tuners (FE-FRTs) are a novel type of tuner that may be able to achieve near perfect compensation of microphonics in the near future. This would eliminate the need to design over-coupled fundamental power couplers and thus significantly reduce RF power, particularly for low beam current applications.

The recently tested proof of principle FE-FRT is discussed and the theory and practice of FE-FRT operation are developed. These theoretical methods are then used to explore the potential benefits of using an FE-FRT with specific ERL proposals, which are seen as one of the major use cases. Specifically the ERLs considered are: eRHIC ERL, PERLE, LHeC ERL and the Cornell Light Source. Particular attention is given to the substantial peak and average RF power reductions which could be achieved; in many cases these are shown to be approximately an order of magnitude.

INTRODUCTION

Energy Recovery Linacs (ERLs) are designed to operate with virtually no beam loading. In principle, the only forward power that must be supplied to an ERL cavity is that needed to replace the power lost on the cavity walls. For superconducting cavities this is rather small.

Unfortunately, even with well designed cryomodules, frequency excursions caused by microphonics are typically orders of magnitude larger than the natural bandwidth of the cavity and as a result almost all of the supplied forward power is reflected and lost.

Significant effort has been made in recent years to design fast mechanical piezo-electric tuners to combat microphonics. Whilst important progress has been made in this direction[1–3], it is an extremely difficult challenge. Although piezo-electric crystals are intrinsically fast, the speed of a piezo-electric tuner is limited by how fast a deformation can be applied to the cavity wall. A cavity also has its own mechanical resonances which imply complicated transfer functions between piezo actuator input and cavity resonant frequency. In addition, any applied mechanical deformation will invariably excite additional unwanted mechanical vibrations which will themselves affect the frequency.

Recent progress in ferroelectric (FE) material properties[4–6] have now made an entirely new method of combat-

ting microphonics viable. An FE-FRT is a device containing FE material which is coupled to the cavity via an antenna and transmission line. By applying a voltage to the FE, its permittivity and therefore the reactance coupled to the cavity is altered, which changes the cavity's resonant frequency.

FE-FRTs have no moving parts, do not act on the cavity mechanically and do not excite unwanted mechanical vibrations. They also operate outside of cryomodules avoiding the cryogenic cost of dissipating power in liquid helium.

For ERLs and low beam loading machines FE-FRTs could soon offer significant power and cost savings.

PROTOTYPE FE-FRT

A proof of principle (PoP) FE-FRT was designed by S. Kazakov, built by Euclid and successfully tested on an SRF cavity at CERN[7]. A photograph and 3D rendering are shown in Fig. 1. It connects to the cavity on the left via a co-axial cable and to a high voltage source on the right.

The PoP FE-FRT was tested with a superconducting cavity and preliminary results were presented in [7]. The (measurement limited) response of the cavity to the tuner was found to be $< 50 \mu\text{s}$, the true response may be much faster as the FE material itself responds in $\sim 10\text{s ns}$ [8, 9].

Whilst the response time estimation was measurement limited, it is already possible to draw two key conclusions. Firstly the cavity response to an FE-FRT is not limited by the time constant of the cavity. Secondly the response time is certainly fast enough to easily correct for microphonics which are typically not significant above $\approx 1\text{kHz}$ [3, 10].

Predictions of PoP FE-FRT impedance as a function of frequency were made with a transmission line model (TLM), and compared to CST simulations[11] and VNA measurements in Fig. 2. Close agreement is seen around the intended operating frequency ($\approx 400\text{ MHz}$), validating the TLM.

MECHANISM OF ACTION

Theory of an FE-FRT has already been presented in [7]. Here the most important results are reviewed and behaviour in anticipated paradigmatic scenarios is explored.

Theoretical Overview

The cavity is modelled as a conductance G_c , capacitance C_c and inductance L_c connected in parallel. The cavity-tuner or FE-FRT coupler is modelled as a lossless trans-

* This work was supported in part by the DOE SBIR grant: DE-SC0007630.

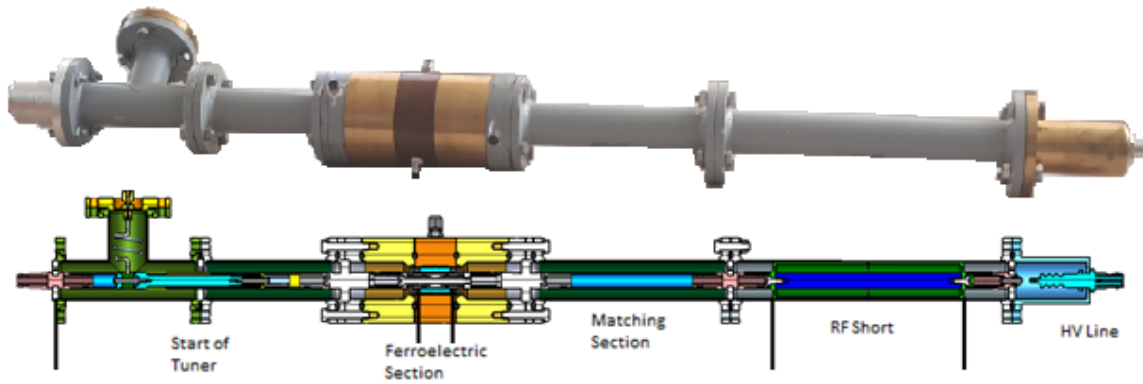
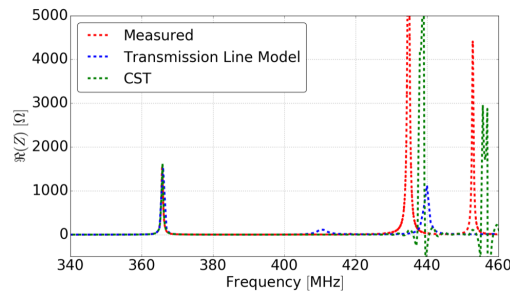
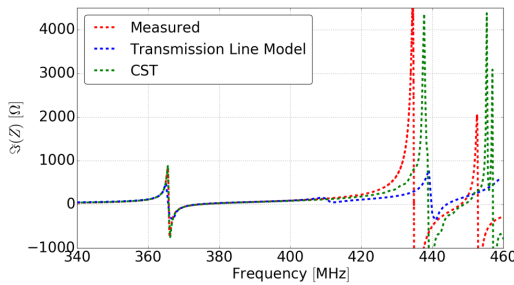


Figure 1: A photograph and cut away 3D rendering of the PoP FE-FRT.



(a) Real part of impedance.



(b) Imaginary part of impedance.

Figure 2: Impedance of the PoP FE-FRT vs. frequency measured with a VNA (red); derived from a Transmission Line Model (blue); and simulated with CST (green).

former of ratio N . The tuner and transmission line (TL) connecting it to the cavity, has an admittance Y'_t ; with real and imaginary parts G'_t (conductance) and B'_t (susceptance) respectively.

The tuner admittance as seen by the cavity is:

$$Y_t = G_t + iB_t = \frac{Y'_t}{N^2} \quad (1)$$

A prime indicates a tuner quantity before it is 'coupled into the cavity' through the transformer. A subscript can indicate the corresponding tuner state¹[7], with ' n ' denoting an arbitrary state and '1' and '2' denoting the 'end' states with minimum and maximum FE permittivities respectively.

Table 1 shows the theoretical expressions developed in [7]. $\Delta\omega_{12}$ is the tuning range effected by the FE-FRT, with $\Delta B'_{t12}$ the change in FE-FRT susceptance between the

¹ The state of an FE-FRT, for example, would be different for different FE permittivities resulting from voltages applied to it.

Table 1: Review of Theoretical Results

Description	Symbol	Equation
Tuning range	$\Delta\omega_{12}$	$\frac{-\omega_0 \Delta B'_{t12} \sqrt{L_c/C_c}}{2N^2}$
Dissipated Power	P_{tn}	$U_c \frac{G'_{tn}}{N^2 C_c}$
Reactive Power	\mathcal{P}_{tn}	$U_c \frac{B'_{tn}}{N^2 C_c}$
Increase in Bandwidth	ΔBW_n	$\frac{G'_{tn}}{N^2 C_c}$
State Ratio	SR_n	$\frac{\Delta\omega_{12}}{\Delta BW_n}$
Figure of Merit	FoM	$\frac{2 \sin \frac{\Delta\theta_{12}}{2} }{\sqrt{(1- \Gamma_1 ^2)(1- \Gamma_2 ^2)}}$

states. P_{tn} and \mathcal{P}_{tn} are the dissipated and reactive power in the FE-FRT, with U_c the cavity's stored energy. ΔBW_n is the increase in cavity bandwidth due to the FE-FRT. SR_n is the 'State Ratio' and FoM the 'Figure of Merit'. Γ_1 and Γ_2 are the reflection coefficients in states 1 and 2 respectively and $\Delta\theta_{12}$ the difference in phase between them.

SR_n can be calculated from equivalent circuit parameters and enables the calculation of ΔBW_n from $\Delta\omega_{12}$ independent of N . As it depends on the state and TL length, it is not a useful figure of merit, which we instead define as the geometric average of SR_1 and SR_2 . The FoM allows easy comparison of different FE-FRT designs via simulation and evaluation of FE-FRT performance via VNA measurements. A higher FoM gives greater tuning range with reduced losses.

Examples of Operation

The theory in the previous section is now used to study different operational scenarios for a hypothetical cavity and FE-FRT operating at 800 MHz. Figure 3 shows the Smith chart position, frequency change and the dissipated and reactive power in the FE-FRT vs. FE permittivity, for three TL lengths. For each TL length the coupling ratio N is chosen such that $\Delta\omega_{12}$ is 100Hz.

In the 'Open' scenario the TL length is such that possible Γ_n s are centered on the Smith chart's open position. In this scenario \mathcal{P}_{tn} is minimised. P_{tn} varies slightly between

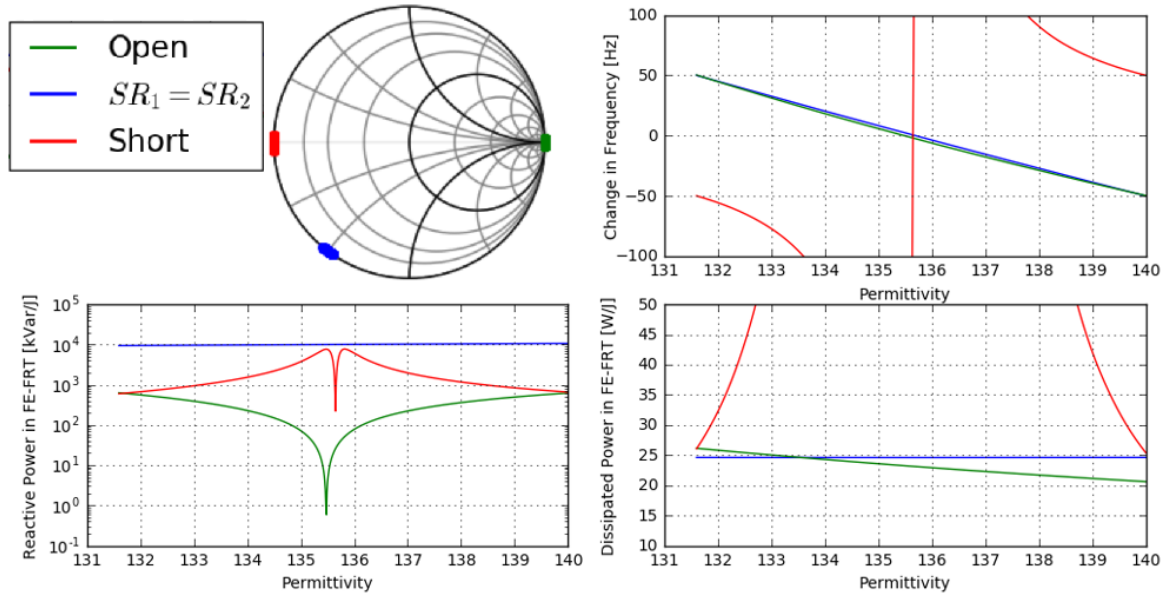


Figure 3: Operational scenarios for three TL lengths. Each antenna is chosen so the frequency shift between end states is 100 Hz. Smith chart position is shown top left. The frequency change (relative to central tuning frequency), dissipated, and reactive power in the FE-FRT vs. FE permittivity are shown top right, bottom left and bottom right respectively.

states, and therefore the cavity loaded-Q (Q_L) and required forward power (P_{RF}) also show a slight variation. This position also requires the most strongly coupled FE-FRT antenna which means the antenna will protrude further into the cavity and see increased losses on its surface. This is still likely to be close to the optimal scenario in the majority of use cases.

In the ‘SR₁ = SR₂’ scenario the TL length is such that SR₁ and SR₂ are equal. In this case, as seen in Fig. 3 the dissipated power is, to a good approximation, state independent. This is an attractive feature as both Q_L and P_{RF} are then also only weakly dependent on the FE-FRT state. However in this scenario the reactive power is large which may be a precluding factor for high U_c or $\Delta\omega_{12}$ applications.

In the ‘Short’ scenario the possible Γ_{ns} are centered on the Smith chart’s short position. As ΔB_{12} is greatest here, this scenario requires the weakest antenna coupling. However, G_{tn} and B_{tn} diverge at the short, resulting in large variations of ω_n , P_{tn} and P_{tn} rendering continuous tuning impossible. This scenario could only be used for switching between two distinct frequencies. Note: reducing the permittivity range diminishes performance; the frequency shift is larger, but the dissipated power is larger still which decreases the FoM.

Table 2 shows the TL length and Q_{eq} of the FE-FRT antenna for each scenario in Fig. 3. We define Q_{eq} as the external Q-factor (Q_e^{FRT}) the antenna would have if terminated by a 50 Ω load. As the impedance of the FE-FRT is usually far from 50 Ω , Q_{eq} is far from Q_e^{FRT} . However, Q_{eq} gives a good intuitive idea of the required antenna size for readers more familiar with Q-factors than coupling ratios.

Table 2: Example Tuner Setup vs. Smith Chart Position

Position	Q_{eq}	Line Length
Open	1.26×10^5	0.283λ
SR ₁ = SR ₂	1.01×10^6	0.475λ
Short	2.94×10^8	0.533λ

APPLICABILITY TO ERLS

As an ERL has almost no beam loading, the forward RF power required to maintain the cavity voltage is [12]:

$$P_{RF} = \frac{V_c^2}{4R/Q} \frac{\beta+1}{\beta} \left[1 + \left(2Q_L \frac{\Delta\omega_\mu}{\omega_0} \right)^2 \right] \quad (2)$$

With no FE-FRT, the Q_L of an ERL cavity is dominated by the external Q-factor of the fundamental power coupler (Q_e). In this case it can be shown from Eq. (2) that the optimal Q_e (Q_e^{opt}) to minimise the peak forward power (P_{RF}^{peak}) is:

$$Q_e^{\text{opt}} \approx \frac{\omega_0}{2\Delta\omega_\mu^{\text{peak}}} \quad (3)$$

where $\Delta\omega_\mu^{\text{peak}}$ is the peak detuning due to microphonics. From Eq. (3) and Eq. (2) it can be shown that if $Q_e = Q_e^{\text{opt}}$:

$$P_{RF}^{\text{peak}} \approx U\Delta\omega_\mu^{\text{peak}} \quad (4)$$

If microphonics induced frequency deviations are normally distributed and $\Delta\omega_\mu^{\text{peak}}$ is defined as greater than 5σ ($\Delta\omega_\mu$) then the average forward power is given by:

$$\bar{P}_{RF} \approx \frac{U\Delta\omega_\mu^{\text{peak}}}{2} = \frac{P_{RF}^{\text{peak}}}{2} \quad (5)$$

If an FE-FRT is used, P_{tn} will contribute to Q_L . For full

microphonics compensation $\Delta\omega_{12}$ must be set to $2\Delta\omega_{\mu}^{\text{peak}}$ and in this case, for a realistic FoM, $Q_0 \gg Q_{FRT}$, with:

$$Q_{FRT} = \frac{\omega_0}{\Delta BW} \quad (6)$$

and ΔBW is defined as:

$$\Delta BW = \sqrt{\Delta BW_1 \Delta BW_2} \quad (7)$$

We assume the tuner is not in the ‘Short’ scenario and:

$$\Delta BW_1 \approx \Delta BW_2 \quad (8)$$

With FE-FRT use as described above $Q_e^{\text{opt}} = Q_{FRT}$ and it can be shown that both peak and average forward power are:

$$P_{RF}^{\text{FRT}} \approx \frac{\omega_0 U}{Q_{FRT}} \approx \frac{2U\Delta\omega_{\mu}^{\text{peak}}}{\text{FoM}} \quad (9)$$

From Eq. (9), Eq. (4) and Eq. (5) it can be seen that:

$$\frac{P_{RF}^{\text{peak}}}{P_{RF}^{\text{FRT}}} \approx \frac{\text{FoM}}{2} \quad (10)$$

and that

$$\frac{\bar{P}_{RF}}{P_{RF}^{\text{FRT}}} \approx \frac{\text{FoM}}{4} \quad (11)$$

An FE-FRT therefore reduces the required peak and average forward power by a factor of $\frac{\text{FoM}}{2}$ and $\frac{\text{FoM}}{4}$ respectively.

FREQUENCY DEPENDENCE OF FOM

The dielectric α_d and conductive α_c losses in a copper coaxial cable at frequency f are given by[13]:

$$\alpha_d = 9.11 \times 10^{-8} f \sqrt{\epsilon_r} \tan \delta \text{ dB/m} \quad (12)$$

$$\alpha_c = 2.98 \times 10^{-7} \sqrt{f} \frac{1}{b} \left(1 + \frac{b}{a}\right) \frac{\epsilon}{\ln \frac{b}{a}} \text{ dB/m} \quad (13)$$

with b and a the outer and inner radii respectively, ϵ_r the relative permittivity of the dielectric and $\tan \delta$ its loss tangent.

The $\tan \delta$ of microwave ceramics including FEs scale linearly with frequency over a wide range of $\approx 100 \text{ MHz} - 100\text{s GHz}$ [5, 14, 15]. If we restrict b such that only the principle TEM mode can propagate, then $b \propto f$ and therefore:

$$\alpha_c \propto f^{3/2} \quad (14)$$

$$\alpha_d \propto f^2 \quad (15)$$

With the above considerations a TLM and Monte-Carlo method similar to that presented in [7] were used to estimate the highest achievable FoM for frequencies between 400 and 1600 MHz. The results are shown in Fig. 4.

CASE STUDIES

The benefit of using an FE-FRT with specific ERL projects is now explored, using the parameter values in table 3. A black font indicates a value taken from a reference[12, 16–21], an orange font a value calculated from a referenced value and a red font an estimated parameter which could neither be found nor calculated from referenced values. Equation (2) is used to calculate all required powers.

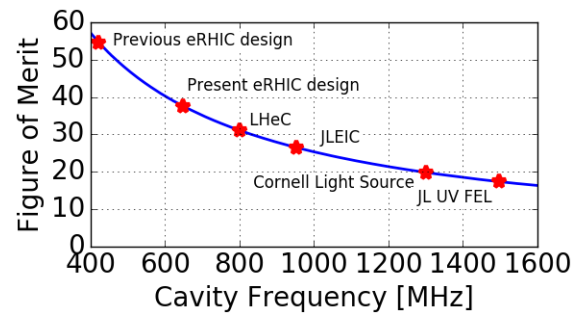


Figure 4: Expected FoM vs. Frequency

For all average powers a normal microphonics distribution is assumed. Also, in the non-FE-FRT case we assume all frequency correction is done via RF power and no other fast tuner (such as a piezo device) is used.

In the FE-FRT case, Q_0 , which forms part of Q_L and β in Eq. (2), is necessarily replaced with the expression: $\frac{1}{Q_0} + \frac{1}{Q_{FRT}}$. The peak and average powers in the FE-FRT case are treated as identical, but this is only strictly true in the ‘SR₁ = SR₂’ scenario. In the ‘open’ scenario for example, the peak power would be $\approx 10\%$ higher than shown.

eRHIC

The eRHIC project[16] recently decided to pursue a Ring-Ring over an ERL based Linac-Ring design. However examining the benefits an FE-FRT could have brought to the ERL design is still informative.

Figure. 4 shows an expected FoM of ≈ 38 at the proposed ERL frequency of 647.4 MHz[22]. No value for the expected microphonics level could be found so a value of 20 Hz was estimated, from which we calculate Q_e based on Eq. (3).

By using an FE-FRT, peak power is reduced by a factor ≈ 19 , and average powers by a factor ≈ 9 . The results are shown in Fig. 5. Both electrical powers assume a grid conversion efficiency of 70 %.

PERLE and LHeC

Both PERLE and the LHeC plan to use an 801.58 MHz cavity[19, 20], whilst several designs exist, here we consider the updated CERN cavity design[21]. At this frequency Fig. 4 gives an expected FoM of ≈ 30 . LHeC appears to use a more optimistic grid conversion efficiency and peak detuning (calculated from the specified total electrical power assuming $Q_e = Q_e^{\text{opt}}$ as per Eq. (3)) than PERLE.

For both PERLE and LHeC, peak power is reduced by a factor ≈ 15 and average power by a factor ≈ 7.5 . The results for PERLE are shown in Fig. 6 and for the LHeC in Fig. 7.

Cornell Light Source

Whilst the ‘maximum’ expected peak detuning for the Cornell Light Source[12] is 20 Hz, Q_e was optimised instead for a ‘typical’ expected peak detuning of 10 Hz. This decreases \bar{P}_{RF} but increases P_{RF}^{peak} . As a consequence, an FE-FRT decreases the average and peak power by a smaller (≈ 3) and greater (≈ 12) factor respectively than shown in Eq. (10) and Eq. (11). The results are shown in Fig. 8

Table 3: Machine Parameters

Parameter	eRHIC	PERLE	LHeC	Cornell
Frequency	647.4 MHz	801.58 MHz	801.58 MHz	1.3 GHz
Cavity Voltage – V_c	26.88 MV	18.7 MV	18.7 MV	13.1 MV
External Q-Factor of FPC – Q_e	1.60×10^7	1.00×10^7	1.56×10^7	6.5×10^7
Intrinsic Q-Factor – Q_0	2.00×10^{10}	2.00×10^{10}	2.00×10^{10}	2.00×10^{10}
R/Q	502 Ω	393 Ω	393 Ω	387 Ω
Peak Detuning – $\Delta\omega_{\mu peak}$	20.0 Hz	40.0 Hz	26.2 Hz	20.0 Hz
RMS Detuning – $\sigma(\Delta\omega_{\mu})$	3.33 Hz	6.67 Hz	4.36 Hz	3.33 Hz
Accelerating Gradient – E_{acc}	16 MV/m	20 MV/m	20 MV/m	16.2 MV/m
Cavity Length	1.68 m	0.935 m	0.935 m	0.81 m
Final Beam Energy	20 GeV	0.9 GeV	60 GeV	5 GeV
ERL Passes	12	3	3	1
Number of Cavities	62	16	1069	384
Grid to RF conversion efficiency	$\approx 70\%$	$\approx 50\%$	$\approx 70\%$	$\approx 50\%$
Total Electrical Power for microphonics control	1.37 MW	732 kW	22.2 MW	734 kW

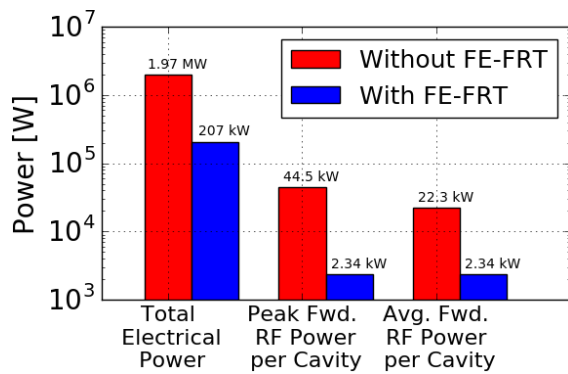


Figure 5: Power savings with FE-FRT use for eRHIC.

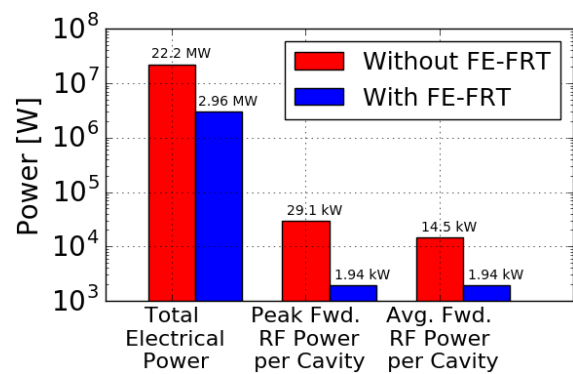


Figure 7: Power savings with FE-FRT use for LHeC.

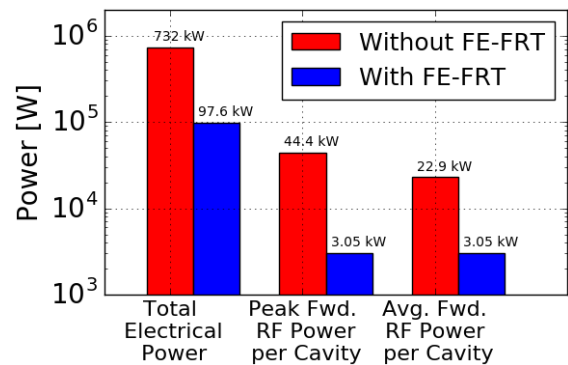


Figure 6: Power savings with FE-FRT use for PERLE.

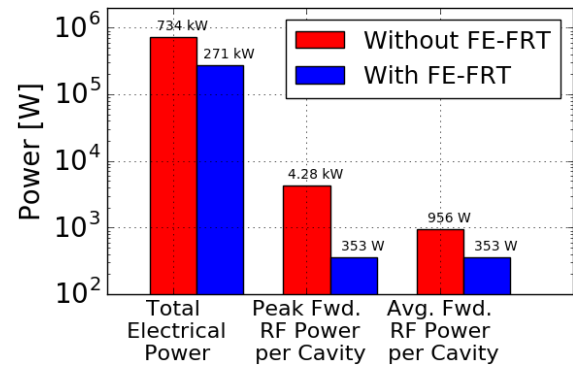


Figure 8: Power savings with FE-FRT use for Cornell.

CONCLUSION

The measured speed at which an FE-FRT can change a cavity’s frequency is fast enough to easily correct for microphonics, but full microphonics compensation must still be verified experimentally. In addition, for future FE-FRT development, losses on the FE brazing must be addressed, as presently these cause a rather low FoM for the PoP FE-FRT. If these two key criteria can be demonstrated however, FE-FRTs would offer power and cost savings for ERLs to an extent that could significantly affect the feasibility and financial viability of large scale projects.

FE-FRTs require their own port and a large coupler which can handle sizeable reactive power, however the cost of implementing this would likely be more than offset by: a large reduction in required grid power; and a decrease in size and cost of RF infrastructure and fundamental power couplers.

FE-FRTs are likely to have a significant impact on a project’s parameter optimisation considerations (for instance operating frequency and cavity design) and would ideally therefore be ‘designed in’ from the beginning.

Content from this work may be used under the terms of the CC BY 3.0 licence (© 2019). Any distribution of this work must maintain attribution to the author(s), title of the work, publisher, and DOI

REFERENCES

- [1] N. Banerjee, G. Hoffstaetter, M. Liepe, P. Quigley, and Z. Zhou, "Active suppression of microphonics detuning in high Q_L cavities," *Physical Review Accelerators and Beams*, vol. 22, pp. 052002–17, 2019. doi: 10.1103/PhysRevAccelBeams.22.052002.
- [2] Y. Pischalnikov *et al.*, "Operation of an SRF Cavity Tuner Submerged into Liquid Helium," in *FERMILAB-CONF-19*, 2019. <https://lss.fnal.gov/archive/2019/conf/fermilab-conf-19-294-td.pdf>
- [3] A. Neumann, W. Anders, O. Kugeler, and J. Knobloch, "Analysis and active compensation of microphonics in continuous wave narrow-bandwidth superconducting cavities," *Physical Review Special Topics - Accelerators and Beams*, vol. 13, no. 8, 2010. doi: 10.1103/PhysRevSTAB.13.082001.
- [4] A. B. Kozyrev, A. D. Kanareykin, E. A. Nenasheva, V. N. Osadchy, and D. M. Kosmin, "Observation of an anomalous correlation between permittivity and tunability of a doped ferroelectric ceramic developed for microwave applications," *Appl. Phys. Lett.*, vol. 95, p. 12908, 2009. doi: 10.1063/1.3168650.
- [5] E. Nenasheva *et al.*, "Low loss microwave ferroelectric ceramics for high power tunable devices," *Journal of the European Ceramic Society*, vol. 30, no. 2, pp. 395–400, Jan. 2010, ISSN: 09552219. doi: 10.1016/j.jeurceramsoc.2009.04.008.
- [6] A. Kanareykin, S. Kazakov, A. Kozyrev, E. Nenasheva, and V. Yakovlev, "Ferroelectric based high power tuner for L-band accelerator applications," in *Proc. IPAC13*, Shanghai: JACoW, paper: WEPWO082, 2013, pp. 2486–2488.
- [7] N. Shipman *et al.*, "A Ferroelectric Fast Reactive Tuner for Superconducting Cavities," in *SRF2019*, Dresden, paper: WETEB7, 2019.
- [8] A. Kanareykin *et al.*, "Fast switching ferroelectric materials for accelerator applications," *AIP Conference Proceedings*, vol. 877, no. December 2006, pp. 311–319, 2006, ISSN: 0094243X. doi: 10.1063/1.2409151.
- [9] S. Y. Kazakov, S. V. Shchelkunov, V. P. Yakovlev, A. Kanareykin, E. Nenasheva, and J. L. Hirshfield, "Fast ferroelectric phase shifters for energy recovery linacs," *Physical Review Special Topics - Accelerators and Beams*, vol. 13, no. 11, p. 113501, Nov. 2010, ISSN: 1098-4402. doi: 10.1103/PhysRevSTAB.13.113501.
- [10] S. Simrock, "Control of Microphonics and Lorentz Force Detuning with a Fast Mechanical Tuner," in *Proc. SRF 2003*, Lübeck, 2003, 254–257, paper: TUO09.
- [11] *CST Studio Suite*. <https://www.3ds.com/products-services/simulia/products/cst-studio-suite/>
- [12] E. G. H. Hoffstaetter *et al.*, "Cornell Energy Recovery Linac Science Case and Project Definition Design Report," Cornell, Tech. Rep., 2013, p. 518.
- [13] T. Moreno, *Microwave Transmission Design Data*, ser. Dover books on physics, engineering. McGraw-Hill Book Company, 1948.
- [14] J. Petzelt and S. Kamba, "Submillimetre and infrared response of microwave materials: Extrapolation to microwave properties," *Materials Chemistry and Physics*, 2003. doi: 10.1016/S0254-0584(02)00269-9.
- [15] J. L. Hirshfield, "Fast 704 MHz Ferroelectric Tuner for Superconducting Cavities," Chicago Operations Office, Argonne, IL (United States), Tech. Rep., Apr. 2012, pp. 1–34. doi: 10.2172/1038253.
- [16] E. C. Aschenauer *et al.*, "eRHIC Design Study: An Electron-Ion Collider at BNL," Tech. Rep., Sep. 2014. arXiv:1409.1633[physics.acc-ph]
- [17] W. Xu *et al.*, "RF and Mechanical Design of 647 MHz 5-CELL BNL4 Cavity for ERHIC ERL," in *Proceedings of IPAC2016*, Busan, 2014. doi: 10.18429/JACoW-IPAC2016-WEPMR041.
- [18] W. Xu *et al.*, "Progress of 650 MHz SRF cavity for eRHIC SRF linac," in *18th International Conference on RF Superconductivity*, Lanzhou: JACoW Publishing, 2017, pp. 64–66. doi: 10.18429/JACoW-SRF2017-MOPB009.
- [19] D. Angal-Kalinin *et al.*, "PERLE. Powerful energy recovery linac for experiments. Conceptual design report," *Journal of Physics G: Nuclear and Particle Physics*, vol. 45, no. 6, p. 065003, Jun. 2018. doi: 10.1088/1361-6471/aaa171.
- [20] J. L. Abelleira Fernandez *et al.*, "A Large Hadron Electron Collider at CERN Report on the Physics and Design Concepts for Machine and Detector," *Journal of Physics G: Nuclear and Particle Physics*, vol. 39, no. 7, p. 075001, Jul. 2012. doi: 10.1088/0954-3899/39/7/075001.
- [21] R. Calaga, "A design for an 802 MHz ERL Cavity," no. CERN-ACC-NOTE-2015-0015, 2015.
- [22] W. Xu, I. Ben-Zvi, T. Roser, and V. Ptitsyn, "Frequency choice of eRHIC SRF linac," Brookhaven National Laboratory (BNL), Upton, NY (United States), Tech. Rep., Jan. 2016. doi: 10.2172/1335380.